The Astrophysical Journal, 670: L85–L88, 2007 December 1

A GIANT RADIO JET EJECTED BY AN ULTRAMASSIVE BLACK HOLE IN A SINGLE-LOBED RADIO GALAXY

Joydeep Bagchi,[1] Gopal-Krishna,[2] Marita Krause,[3] and Santosh Joshi[1,4]

Received 2007 July 5; accepted 2007 October 8; published 2007 October 30

ABSTRACT

We report the discovery of a very unusual, highly asymmetric radio galaxy whose radio jet, the largest yet detected, emits strongly polarized synchrotron radiation and can be traced all the way from the galactic nucleus to the hot spot located ~440 kpc away. This jet emanates from an extremely massive black hole ($>10^9\ M_\odot$) and forms a strikingly compact radio lobe. No radio lobe is detected on the side of the counterjet, even though it is similar to the main jet in brightness up to a scale of tens of kiloparsecs. Thus, contrary to the nearly universal trend, the brightness asymmetry in this radio galaxy *increases* with distance from the nucleus. With several unusual properties, including a predominantly toroidal magnetic field, this Fanaroff-Riley type II megajet is an exceptionally useful laboratory for testing the role of magnetic field in jet stabilization and radio lobe formation.

Subject headings: galaxies: active — galaxies: ISM — galaxies: jets — radio continuum: galaxies

Online material: color figure

1. INTRODUCTION

Radio sources associated with Abell clusters of galaxies are usually weak radio emitters but present a great diversity of morphologies. During a search for radio emission from rich clusters, we noticed a radio source toward Abell 2040, which is associated with a bright $B \sim 14.5$ elliptical galaxy CGCG 049−033 offset from the cluster center by ~22′ (1.1 Mpc, taking $H_0 = 71$ km s^{-1} Mpc^{-1}, $\Omega_M = 0.27$, $\Omega_\Lambda = 0.73$). The redshift $z = 0.04464$ of this galaxy is close to $z = 0.04564$ of the (radio-quiet) central galaxy (UGC 09767) of the cluster (Wegner et al. 1999). In the VLA NVSS database (Condon et al. 1998) we noticed that CGCG 049−033 coincides with a predominantly one-sided radio source, elongated on 10′ scale (~0.5 Mpc), but its structural details remained poorly defined due to the modest resolution (45″). In view of its potentially huge size we have imaged the radio source, as well as taken its optical spectrum. Our observations have revealed the source to be highly unusual in terms of radio size, morphology, and polarization, and in being powered by an extremely massive black hole.

2. OBSERVATIONS

2.1. *GMRT Radio Observations (Aperture Synthesis)*

The GMRT[5] observations were made at 1.28 GHz ($\lambda = 23.4$ cm) using the 128 channel correlator of total bandwidth 16 MHz (Swarup et al. 1991). A sequence of 30 minute scans of the source was taken on 2004 July 15, interspersed with the phase calibrator 1445+099. The telescope gain and the bandpass were calibrated using 3C 286. After excising bad data and RFI, the calibrated data were transformed into the image plane using the standard routines in AIPS, including a few cycles of self-calibration. By applying suitable tapers to the visibilities, two maps with synthesized Gaussian beams of FWHM 3″ and 11″ were obtained (Fig. 1). The 11″ resolution map (dynamic range ~500) shows a pair of well-aligned, collimated jets emanating from an unresolved core (92 mJy, <3″) and extending over 675″ (= 578 kpc). Only the longer southern jet can be traced up to its termination where it forms a hot spot and a remarkably compact radio lobe. Neither the terminal point of the (northern) counterjet nor its lobe are detected, implying a flux density ratio of at least 20 between the southern lobe and any morphologically similar northern lobe. Details of the inner ~2′ region can be seen on the 3″ resolution GMRT map (Fig. 1).

2.2. *Effelsberg Radio Observations (Single-Dish)*

The source was mapped at 8.35 GHz ($\lambda = 3.6$ cm) with the 100 m Effelsberg telescope in 2004 May and July,[6] yielding both total power and polarimetric images (Fig. 2). The single-beam receiver has two channels with total-power amplifiers and an IF polarimeter, at a bandwidth of 1.1 GHz. For pointing, focusing, and flux calibration, 3C 286 was used. A total of 31 coverages of the field were taken by scanning along and perpendicular to the jet. The standard data reduction procedure (Emerson & Gräve 1988) has led to a 20′ × 10′ map, with a Gaussian beam of FWHM 84″ and an rms noise of ~260 μJy beam^{-1} in total power and ~100 μJy beam^{-1} in linear polarization. Despite the large beam averaging, an extraordinarily high linear polarization ($p = 20\%$–50%, average 30%) is found along each jet (Fig. 2).

Further, combining our Effelsberg data with the 1.4 GHz NVSS linear polarization map (Fig. 2; Condon et al. 1998), we obtained the Faraday rotation measure (RM), which was found to vary smoothly in the range ~10 to 40 rad m^{-2}. These RMs were used to correct the observed polarization vectors at 8.35 GHz and thus derive (after a 90° rotation) the projected magnetic field vectors. The magnetic fields of both jets are predominantly transverse to their axes (Fig. 2). Note that these vectors should be intrinsic to the source because foreground RM is negligible, as estimated from the known RMs of eight

[1] Inter-University Centre for Astronomy and Astrophysics (IUCAA), Pune University Campus, Post Bag 4, Pune 411007, India; joydeep@iucaa.ernet.in.

[2] National Centre for Radio Astrophysics, TIFR, Pune University Campus, Post Bag 3, Pune 411007, India.

[3] Max-Planck-Institut für Radioastronomie, Auf dem Hügel 69, 53121 Bonn, Germany.

[4] Aryabhatta Research Institute of Observational Sciences (ARIES), Manora Peak, NainiTal 263129, India.

[5] The GMRT is a national facility operated by the National Centre for Radio Astrophysics of the TIFR, India.

[6] Based on observations with the 100 m telescope of the MPIfR (Max-Planck-Institut für Radioastronomie) at Effelsberg on behalf of the Max-Planck-Gesellschaft.

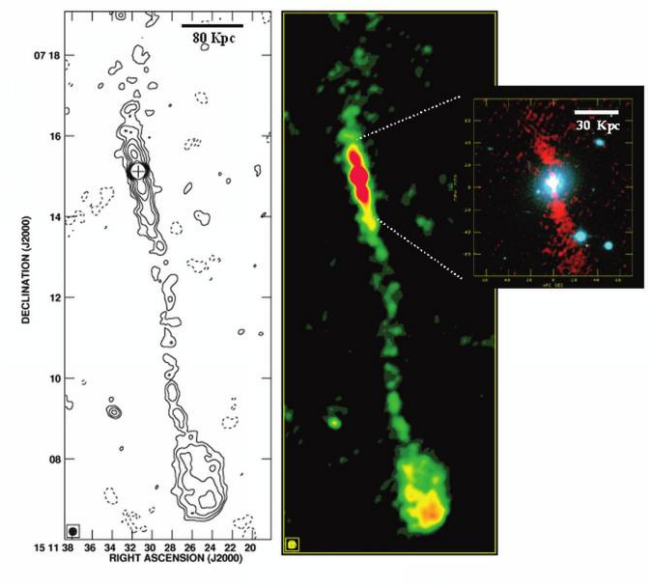

FIG. 1.—GMRT maps at 1.28 GHz, showing intensity contours −0.18, 0.18, 0.36, 0.72, 1.44, 3, and 6 mJy beam^{-1} (*left*), rms noise ~60 μJy beam^{-1}, and the pseudocolor image (*center*), both with a 11″ beam. The details of the inner ~ 2′ region (*inset*) are visible in the 3″ resolution 1.28 GHz GMRT image (*shown in red*) overlaid on the optical *r*-band SDSS image (*shown in blue*).

background sources projected near CGCG 0049−033 (Simard-Normandin et al. 1981).

Remarkably, even in this single-dish observation—more sensitive to diffuse emission—no trace of a northern lobe is found, down to a sensitivity limit of ~1 mJy beam^{-1}. Nonetheless, the counterjet is clearly detected, albeit only marginally resolved with the 84″ beam.

2.3. *Optical Spectroscopy*

Since an existing optical spectrum of CGCG 0049−033, taken with the 2.4 m Hiltner telescope at Kitt Peak, did not cover the wavelength of any prominent emission line (Fig. 2; M. Colles 2007, private communication), we used the newly commissioned 2 meter telescope of IUCAA, equipped with the IUCAA Faint Object Spectrograph and Camera (IFOSC), together with grism 7 (600 grooves mm^{-1}), to cover a wider spectral range 3800–6840 Å. A single 15 minute exposure was taken through a 1.5″ wide slit centered on the galaxy. For data reduction the IRAF package and for wavelength calibration the He-Ne arc lamp standard were used. The reduced spectrum (spectral dispersion 1.4 Å pixel^{-1}) confirms the strong absorption lines of Mg I *b* and Na D of the Kitt Peak spectrum and also shows the H_β, Ca+Fe *E* band and the TiO absorption features (Fig. 2). However, the emission line [O III] 5007 Å remained undetected and thus still provides no hint of AGN activity. A Gaussian fit to the Na D (5893 Å) line gives a very large stellar velocity dispersion $\sigma_* = 375 \pm 35$ km s^{-1}, after correcting for the instrumental broadening. This is consistent with the Kitt Peak value $\sigma_* = 353 \pm 60$ km s^{-1} (Wegner et al. 1999).

3. RESULTS

Data on all 660 extragalactic radio jets known until 2000 December (Liu & Zhang 2002) and the subsequent literature reveals that the main jet of CGCG 0049−033, with a projected length ~440 kpc, is the largest known astrophysical jet, seen stretching all the way from the nucleus to its terminal hot spot. In physical (projected) extent, it is ~7 times the bright jet of the unique one-sided quasar 3C 273 (Conway et al. 1993) and nearly 2 times longer than the jet of the giant radio galaxy NGC 6251 (Willis et al. 1982). From Figure 1, despite the rather limited resolution transverse to the jet, there is a strong hint of its helical morphology. Also evident is the jet's wiggle on the scale of ~300 kpc after the initial ~30″ (~25 kpc) length, up to which point both the jet and counterjet are probably well within the ISM of the host galaxy and both remain straight, well aligned, and similar in apparent brightness (typical contrast ~1.3). But whereas the main jet remains collimated and forms a lobe, the counterjet undergoes an abrupt fading, as indicated by the nondetection of its radio lobe (Figs. 1 and 2).

Integrated flux densities of the source are 208 ± 10, 200 ± 15, and 104 ± 10 mJy at 1.28 GHz (GMRT), 1.4 GHz (NVSS), and 8.35 GHz (Effelsberg), respectively. The spectral index values (α; $S_\nu \propto \nu^{-\alpha}$) are 0.23, 0.50, 0.58, and 0.37 for the core, jet, lobe, and the integrated emission, respectively, obtained by comparing the NVSS map (1.4 GHz, smoothed to 84″) and Effelsberg map (8.35 GHz)—the two being most sensitive to extended emission.

Note that the integrated luminosity (8.8×10^{30} ergs s^{-1} Hz^{-1} at 1.4 GHz) falls nearly 2 orders of magnitude below the Fanaroff-Riley transition (Fanaroff & Riley 1974), making the FR II morphology of this jet very unusual. However, an FR I pattern characterized by jet symmetry is indeed present on the inner 10 kpc scale, based on the jet symmetry (Fig. 1).

We now highlight a few other striking properties of the present source that, when taken together, set it apart from nearly all the known FR II radio galaxies.

1. A supermassive central black hole is revealed by the very large stellar velocity dispersion $\sigma_* = 375 \pm 35$ km s^{-1} (§ 2.3). Following Tremaine et al. 2002,

$$\log (M_{\rm BH}/M_\odot) = \alpha + \beta \log (\sigma_*/\sigma_{200}), \quad (1)$$

where $\sigma_{200} = 200$ km s^{-1} and $\alpha = 8.13 \pm 0.06$, $\beta = 4.02 \pm 0.32$. This gives for CGCG 049−033 ($\sigma_* = 353$ km s^{-1}) a black hole mass $M_{\rm BH} = 1.32 \pm 0.93 \times 10^9 M_\odot$.

An independent estimate of $M_{\rm BH}$ is obtained using the following relation (Marconi & Hunt 2003):

$$\log (M_{\rm BH}/M_\odot) = a + b(\log L_{K,\,\rm bulge} - 10.9), \quad (2)$$

where $L_{K,\,\rm bulge}$ is the bulge luminosity in *K*band (2.17 μm) in solar units $L_{K,\odot}$, and $a = 8.21 \pm 0.07$, $b = 1.13 \pm 0.12$. Since there is no indication of a disk component in CGCG 0049−033 (SDSS; York et al. 2000), its *K*-band absolute magnitude ($M_K = -26.22 \pm 0.044$) from the 2MASS data (Skrutskie et al. 2006) gives its bulge emission: $L_{K,\,\rm bulge} = 6.5 \times 10^{11} L_{K,\odot}$. The resulting $M_{\rm BH} = (1.73 \pm 0.51) \times 10^9 M_\odot$, is close to the above estimate using equation (1). The average of the two, $M_{\rm BH} = (1.5 \pm 1) \times 10^9 M_\odot$, falls in the league of most massive nuclear black holes known [e.g., the radio galaxy M87, with $M_{\rm BH} = (2.4 \pm 0.7) \times 10^9 M_\odot$ (Harms et al. 1994), and also the quasar 1745+624 (Cheung et al. 2006)].

2. The observed strong linear polarization and its orientation imply a well-organized transverse (toroidal) magnetic field for this giant FR II jet, which, in principle, can result from compression of initially tangled magnetic fields in a succession of shocks (Laing 1981). However, the magnetic field in extended FR II jets is typically found to be along the jet (Bridle et al. 1994). Conceivably, in kiloparsec scale jets the dominant contribution to the magnetic field may arise from a

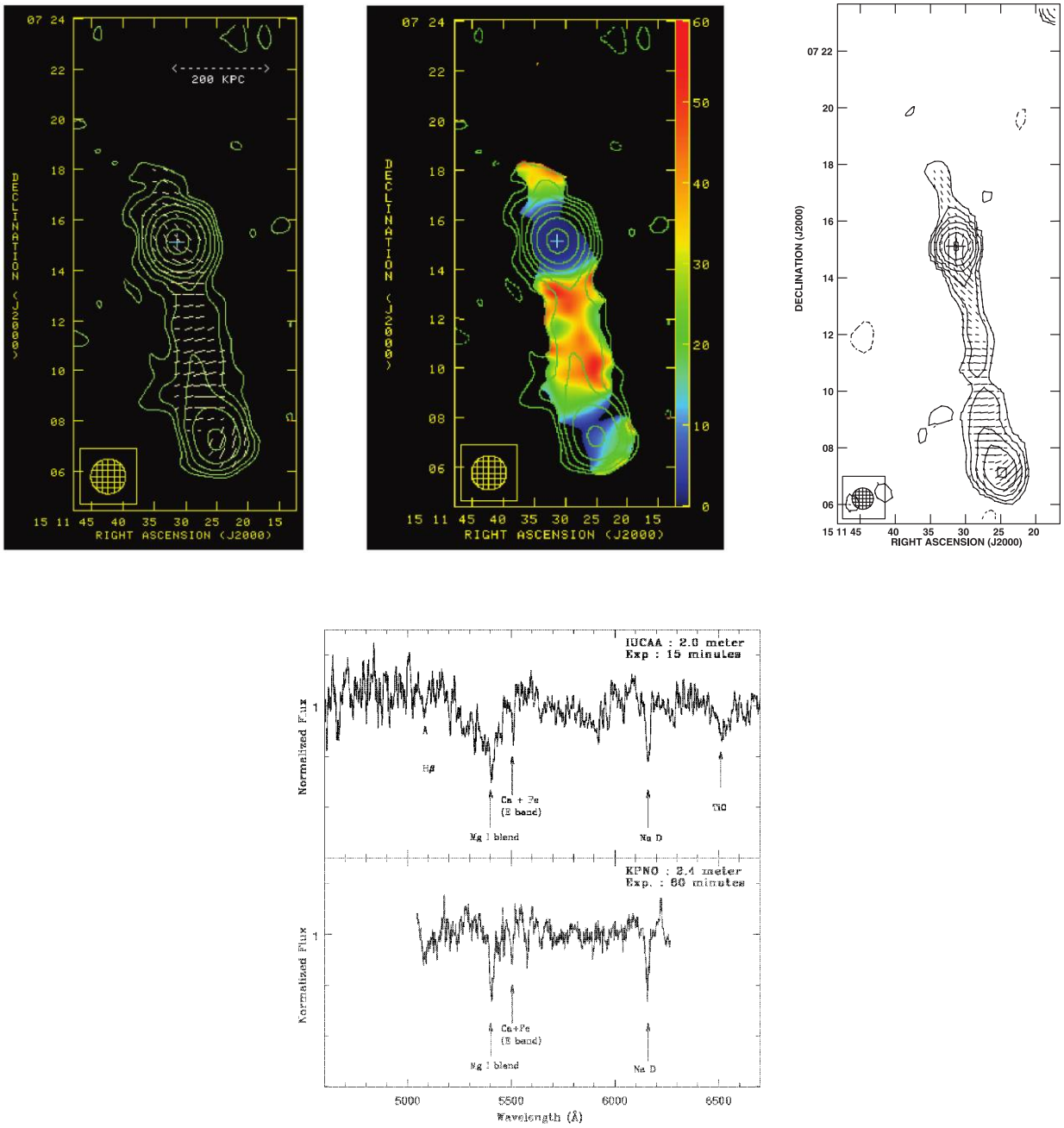

FIG. 2.—*Left*: Effelsberg 8.35 GHz observations of CGCG 049−033 showing total intensity map (contours: −0.75, 0.75, 1.5, 3, 6, 12, 24, and 48 mJy beam^{-1}) along with RM corrected magnetic field vectors (*lines*), having lengths proportional to the local intensity of linearly polarized flux (scale: $1'' = 47.6$ μJy beam^{-1}). *Middle*: Percentage linear polarization at 8.35 GHz shown in pseudocolor, overlaid on the total intensity contours. The HPBW is $84''$ shown inside the box. *Right*: 1.4 GHz NVSS contour map is shown (contours: −1.25, 1.25, 2.5, 5, 10, 20, 40 and 80 mJy beam^{-1}), along with the electric field vectors of linear polarization (scale: $1'' = 0.13$ mJy beam^{-1}). The HPBW is $45''$ shown inside a box. The plus sign marks the radio core at the nucleus of the elliptical galaxy CGCG 049−033 (R.A.$= 15^{h}11^{m}31.38^{s}$, decl.$= 07°15'7.11''$ [J2000.0]). *Bottom*: Optical spectra of CGCG 049−033 taken with IFOSC on the 2 m telescope of IUCAA and with the 2.4 m Hiltner/KPNO telescope (for details, see § 2.3). [*See the electronic edition of the Journal for a color version of this figure.*]

dynamo in the turbulent shear layers (e.g., Matthews & Scheuer 1990; Urpin 2002). The orthogonal magnetic field orientation in the present jet is then also unusual (§ 4).

3. The observed core-to-lobe flux density ratio, $f_c = 1.67$, at 1.28 GHz is an extreme value; for FR II radio galaxies with matching radio lobe power to CGCG 049−033, f_c is typically only ~0.1 (Zirbel & Baum 1995). The large excess in f_c, by a factor $F \sim 17$, could be attributed to relativistic beaming, which can boost the core flux by a factor $\sim\delta^n$ (usually $n \sim 2$ for compact flat-spectrum jets, and the Doppler factor is $\delta = [\Gamma_j(1 - \beta_j \cos\theta)]^{-1}$, where $v_j = c\beta_j$ is the bulk speed of jet and Γ_j, the bulk Lorentz factor). The corresponding viewing angle θ of the nuclear jet (see Giovannini et al. 1994), $\cos(\theta) = [0.5 + (\sqrt{F} - 1)/\beta_j]/\sqrt{F}$, is then quite small ($\theta 28°$ for $\beta_j 1$). Such small angles are jointly disfavored by the projected giant radio size, the apparent symmetry of the inner jets, and the identification with a galaxy (see Barthel 1989).

4. DISCUSSION

The aforementioned peculiarities of CGCG 0049−033 should be viewed in the context of its other striking abnormality, the compactness and apparent one-sidedness of the radio lobe. Note that the counterlobe is undetected down to brightness

contrasts of ~10 and ~15 on the Effelsberg and NVSS maps, respectively (Fig. 2). Indeed, the huge lobe asymmetry together with the symmetry of the inner jets stands in stark contrast to the pattern common for double radio sources (Bridle et al. 1994; Gopal-Krishna & Wiita 2005). We now discuss some possible scenarios for the lobe's unusual properties.

4.1. *The Lobe Asymmetry: Delayed Lobe Formation?*

The appearance of the radio lobe on just one side of the nucleus is reminiscent of the quasar 3C 273, well known for its unique one-sided radio morphology (e.g., Conway et al. 1993), which may even be an artifact of the light travel time effect arising from a combination of small viewing angle ($\theta \sim 10°$–$20°$) and the exceptionally large speed of the jet's head (V_h; e.g., Kundt & Gopal-Krishna 1986; Stawarz 2004).

In CGCG 0049−033, the radio lobe resulting from "backflow" of synchrotron plasma from the hot spot is remarkably compact and well bounded even on the side facing the nucleus. Thus, no lobe is seen around the initial ~80% of the jet's length, giving the source a "pendulum"-like appearance (Fig. 1). Moreover, since the nondetection of the lobe of the counterjet would require it to be intrinsically underluminous compared to the main lobe by an extreme factor ($\gtrsim 20$; § 2), it seems more likely that the northern lobe is hidden due to the light travel-time effects. Thus, a plausible scenario is that the lobe formation in this source began only after the jet had grown to ~80% (i.e., ~350 kpc in projection) of its presently observed length (~440 kpc in projection), possibly due to an unusually prolonged phase of the jet's ballistic propagation.

The observed radio extent ~100 kpc for the counterjet is therefore only a lower limit, because its farthest part could be Doppler-dimmed below the detection threshold. But, in any case, the outer edge of the source on the counterjet side is now being monitored at most at a stage just prior to the onset of lobe formation (otherwise, that lobe too would have been detected). This assumes intrinsic symmetry, which then also implies an upper limit of 350 kpc to the projected extent of the source on the counterjet side (see above). The two limiting values of 100 and 350 kpc correspond to a ratio R between 4.4 and 1.26 of the apparent lengths of the approaching and receding jets, where $R = [1 + (V_h/c) \cos\theta]\,[1 - (V_h/c) \cos\theta]$ (Stawarz 2004).

Therefore, $V_h > c/3$, even if $\theta = 69°$, the median value for FR II radio sources in the unified scheme (Barthel 1989). This is an order of magnitude larger than the typical expansion speed of large radio sources (e.g., Barai & Wiita 2006) but similar to the speed ($V_h \sim 0.85c$) deduced by Stawarz (2004) for the extremely asymmetric quasar 3C 273. Stawarz has proposed that the jet of 3C 273 is propagating through an ultrararified medium of a fossil radio lobe (i.e., cavity) created during a previous episode of nuclear activity. Note that the delayed lobe formation scenario can "hide" the far-side lobe without requiring it to recede at a *bulk* relativistic speed.

4.2. *The Lobe's Compactness*

The lobe's striking compactness could be due to a dynamically important (toroidal) magnetic field associated with the jet, or a well-ordered ambient magnetic field. The latter, too, could assist in jet collimation and formation of a compact radio lobe, as found in the 3D magnetohydrodynamical (MHD) simulations of relativistic jets propagating through a strong magnetic field aligned with the jet (Nishikawa et al. 1997). In the aforementioned scenario of jet propagation through a ghost cavity, such an aligned ambient magnetic field would indeed be expected for the jet (see, e.g., Feretti & Giovannini 2007).

The detection of a highly organized transverse (toroidal) magnetic field in the present jet is exceptional not only for the largest physical scale found thus far, but also for being opposite to the usual pattern exhibited by FR II jets (§ 3). This underscores the importance of this megajet as a rare example where a dynamically important magnetic field is traceable up to several hundred kiloparsecs from the nucleus. Plausibly, the light-travel time and peculiar magnetic configuration internal (or external) to the jet are two rare effects simultaneously at work, leading to its extraordinary nature. Finally, the sequence of radio knots observed at a quasi-regular spacing of ~40 kpc over most of its length (Fig. 1) as well as its excellent collimation make this megajet a prime target for probing jet confinement mechanisms. A deeper radio imaging of this jet could be used to test viability of the theory of jet stabilization upto megaparsec scales, via a spine-sheath type flow (Hardee et al. 2007), or the jet collimation by a surrounding high-pressure ambient medium, leading to a sequence of reconfinement shocks (Komissarov & Falle 1998).

We thank the operations teams of GMRT (NCRA.TIFR), Effelsberg (MPIfR), and Giravali (IUCAA) observatories. We also thank Paul Wiita and Rainer Beck for useful discussions.

REFERENCES

Barai, P., & Wiita, P. J. 2006, MNRAS, 372, 381
Barthel, P. D. 1989, ApJ, 336, 606
Bridle, A. H., et al. 1994, AJ, 108, 766
Cheung, C. C., Stawarz, L., & Siemiginowska, A. 2006, ApJ, 650, 679
Condon, J.J, et al. 1998, AJ, 115, 1693
Conway, R. G., Garrington, S. T., Perley, R. A., & Biretta, J. A. 1993, A&A, 267, 347
Emerson, D. T., & Gräve, R. 1988, A&A, 190, 353
Fanaroff, B. L., & Riley, J. M. 1974, MNRAS, 167, P31
Feretti, L., & Giovannini, G. 2007, preprint (astro-ph/0703494)
Giovannini, G., et al. 1994, ApJ, 435, 116
Gopal-Krishna, & Wiita, P. J. 2005, in 21st Century Astrophysics, ed. S. K. Saha & V. K. Rastogi (New Delhi: Anita), 108 (astro-ph/0409761)
Hardee, P., Mizuno, Y., & Nishikawa, K.-I. 2007, preprint (astro-ph/0706.1916)
Harms, R. J., et al. 1994, ApJ, 435, L35
Komissarov, S. S., & Falle, S. A. E. G. 1998, MNRAS, 297, 1087
Kundt, W., & Gopal-Krishna. 1986, J. Astron. Astroph., 7, 225
Laing, R. A. 1981, ApJ, 248, 87
Liu, F. K., Zhang, Y.H 2002, A&A, 381, 757
Marconi, A., & Hunt, L. K. 2003, ApJ, 589, L21
Matthews, A., & Scheuer, P. A. G. 1990, MNRAS, 242, 623
Nishikawa, K.-I., et al. 1997, ApJ, 483, L45
Simard-Normandin, M., Kronberg, P. P., & Button, S. 1981, ApJS, 45, 97
Skrutskie, M. F., et al. 2006, AJ, 131, 1163
Stawarz, L. 2004, ApJ, 613, 119
Swarup, G., et al. 1991, Curr. Sci., 60, 95
Tremaine, S., et al. 2002, ApJ, 574, 740
Urpin, V. 2002, A&A, 385, 14
Wegner, G., et al. 1999, MNRAS, 305, 259
Willis, A. G., Strom, R. G., Perley, R. A., & Bridle, A. H. 1982, in IAU Symp. 97, Extragalactic Radio Sources, ed. D. S. Heeschen & C. M. Wade (Dordrecht: Reidel), 141
York, D. G., et al. 2000, AJ, 120, 1579
Zirbel, E. L., & Baum, S. A. 1995, ApJ, 448, 521